

STANDARD MODEL HIGGS RESULTS FROM ATLAS AND CMS EXPERIMENTS*

JANA FALTOVA

on behalf of the ATLAS and CMS collaborations

Institute of Particle and Nuclear Physics
Faculty of Mathematics and Physics, Charles University in Prague
V Holešovičkách 2, 180 00 Prague 8, Czech Republic

(Received April 7, 2016)

This paper presents an overview of the current status of Higgs boson measurements from the ATLAS and CMS experiments at the LHC. First, the Higgs boson mass, couplings, CP and spin analyses will be discussed. Proton–proton collisions data at the centre-of-mass energies of 7 TeV and 8 TeV have been used for these studies. Finally, preliminary Higgs boson cross-section measurements at the centre-of-mass energy of 13 TeV are presented.

DOI:10.5506/APhysPolB.47.1459

1. Introduction

The study of the mechanism of the electroweak symmetry breaking is one of the main goals of the ATLAS [1] and CMS [2] detectors at the CERN Large Hadron Collider (LHC). The Englert–Brout–Higgs mechanism [3–5] introduces a complex doublet scalar field to achieve the symmetry breaking. This theory predicts the existence of a neutral scalar boson, commonly called the Higgs boson. The Standard Model (SM) does not predict the mass of the Higgs boson particle. However, with the knowledge of its mass, the production cross section and branching ratios can be calculated. The Higgs boson-like particle discovery was announced by the ATLAS and CMS collaborations in July 2012 [6, 7]. Measurements of its properties have been performed using LHC proton–proton data from years 2011 and 2012 (Run 1). The collision data sets correspond to approximately 5 fb^{-1} at the centre-of-mass energy of $\sqrt{s} = 7 \text{ TeV}$ and 20 fb^{-1} at $\sqrt{s} = 8 \text{ TeV}$. Results from

* Presented at the Cracow Epiphany Conference on the Physics in LHC Run 2, Kraków, Poland, January 7–9, 2016.

Run 1 have shown a good agreement with the predictions of the SM. More precise measurements are planned using new LHC data at the centre-of-mass energy of $\sqrt{s} = 13$ TeV (Run 2). The integrated luminosity usable for physics analyses collected during the first year of Run 2, 3 fb^{-1} contains only a small amount of data compared to Run 1. However, due to the higher centre-of-mass energy, the production cross sections increase with respect to Run 1. Nevertheless, more precise measurements will become possible once more data is available.

The paper is organised as follows: The ATLAS and CMS detectors are briefly introduced in Section 2. The results of the combined measurement of the Higgs boson mass using the ATLAS and CMS experiments are presented in Section 3. The measurements of the Higgs boson production and decay rates, and the constraints on its couplings based on a combined ATLAS and CMS analyses are discussed in Section 4. The results of the Higgs boson spin and CP measurements, as published by the CMS Collaboration, are shown in Section 5. Preliminary Run 2 cross-section measurements using the ATLAS detector are presented in Section 6. The results are summarised in Section 7.

2. ATLAS and CMS detectors

ATLAS and CMS are both multipurpose particle detectors with a cylindrical geometry. One of the important differences between the detectors comes from the magnetic field which defines the size of the detectors. The CMS detector is a compact detector being 21 m long with a diameter of 15 m, whilst the ATLAS detector is a significantly larger apparatus with a length of 46 m and a diameter of 25 m. The magnetic field of ATLAS is formed by a superconducting solenoid providing a 2 T axial magnetic field in the inner tracker and by a system of three large superconducting air-core toroid magnets providing the magnetic field for the muon spectrometer. In contrast, the magnetic field of the CMS detector is formed by a single superconducting solenoid of 6 m internal diameter, providing a magnetic field of 3.8 T. The inner detector and also the calorimeter system are located inside the solenoid.

The ATLAS experiment uses precise silicon detectors (pixel detectors and silicon strips) close to the beam pipe and a transition radiation straw-tube tracker, which is used to enhance the electron identification, in the outer region. The CMS inner detector is based solely on silicon detectors, using pixel detectors in the area closest to the beam pipe and strip trackers in the outer region.

The ATLAS and CMS experiments take advantage of different calorimeter technologies. The CMS calorimeter system is formed by homogeneous lead-tungstate crystal electromagnetic calorimeter and a brass/scintillator

hadron calorimeter. The ATLAS experiment uses sampling calorimeters for both the electromagnetic and hadronic calorimeters. The electromagnetic calorimeter is formed by a highly segmented lead/liquid-argon (LAr) sampling calorimeter. Similar technology is used to measure the hadronic showers in the end-caps (copper/LAr) and to record the electromagnetic and hadronic showers in the forward regions (copper/tungsten/LAr). The hadronic showers in the central region ($|\eta| < 1.7$) are measured using iron/scintillating tile technology.

For ATLAS, the muon spectrometer is placed in the toroidal magnetic field. It is designed to measure muons in the pseudorapidity range up to $|\eta| = 2.7$. Monitored drift-tube chambers and cathode strip chambers are used as precision chambers, whilst resistive plate chambers and thin gap chambers are used as trigger chambers. For the CMS detector, muons are measured in gas-ionization detectors (drift-tube chambers and cathode strip chambers) that are embedded in the steel flux-return yoke outside the solenoid.

3. Higgs boson mass

The Higgs boson mass m_H has been measured independently by the ATLAS and CMS collaborations using proton–proton collisions data from Run 1 in several decay channels. Channels with the best mass resolution ($H \rightarrow \gamma\gamma$ and $H \rightarrow ZZ \rightarrow \ell^+\ell^-\ell'^+\ell'^-$) are used for the combined measurement of the ATLAS and CMS experiments [8] to improve the precision.

The $H \rightarrow \gamma\gamma$ channel can be characterised by a narrow resonance above a large falling background. The typical yields are several hundreds of events as can be seen in figure 1. The main background comes from the SM continuum diphoton production. The photon+jet and dijet production also contribute to the background, especially in the case jet fragments into π^0 s.

The $H \rightarrow ZZ \rightarrow \ell^+\ell^-\ell'^+\ell'^-$ channel, where ℓ, ℓ' stands for an electron or a muon, is denoted as $H \rightarrow ZZ \rightarrow 4\ell$ in the following. In contrast to the previous channel, the yields represent only few tens of events per experiment. The background is very low with a signal-to-background ratio above one. The largest background comes from the continuum $(Z + Z^{(*)})/\gamma^*$ production.

The measurement of m_H and its uncertainty is based on the maximisation of profile-likelihood ratios $\Lambda(\alpha)$ in the asymptotic regime [9, 10]

$$\Lambda(\alpha) = \frac{L(\alpha, \hat{\theta}(\alpha))}{L(\hat{\alpha}, \hat{\theta})}, \quad (1)$$

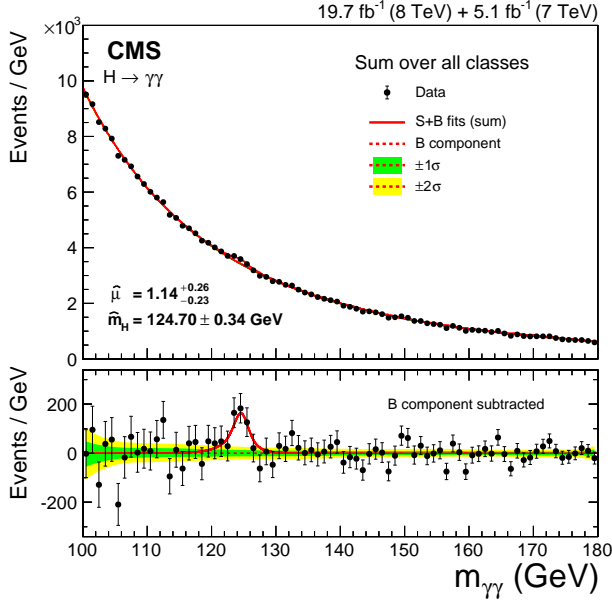


Fig.1. Higgs boson mass measurement in the $H \rightarrow \gamma\gamma$ channel using the CMS detector. Taken from Ref. [11].

where L represents the likelihood function, α the parameters of interest and θ the nuisance parameters. The nuisance parameters are related to the systematic uncertainties, to the fitted parameters of the background models and to any unconstrained signal model parameters. The latter two are incorporated into the statistical uncertainty. The terms $\hat{\alpha}, \hat{\theta}$ denote the unconditional maximum likelihood estimates of the best-fit values for the parameters, while the term $\hat{\theta}(\alpha)$ is the conditional maximum likelihood estimate for a fixed value of α parameter.

In order to make the mass measurement as independent as possible of the SM assumptions, three signal strength parameters have been introduced in the fit. The signal strength is defined as the ratio between the measured cross section times branching ratio and between the corresponding SM expectation. Two independent factors are used in the $H \rightarrow \gamma\gamma$ channel — one for the production processes involving Higgs boson couplings to fermions (gluon fusion and associated production with a top–anti-top pair) and the other one for processes involving couplings to vector bosons (vector boson fusion and associated production with a vector boson). Almost no sensitivity to the production mechanisms other than gluon fusion is observed in the $H \rightarrow ZZ \rightarrow 4\ell$ channel and, therefore, only a single signal-strength parameter is used in this channel.

The Higgs boson mass measurement based on the combination of the ATLAS and CMS results leads to

$$m_H = 125.09 \pm 0.21(\text{stat.}) \pm 0.11(\text{scale}) \pm 0.02(\text{other}) \pm 0.01(\text{theory}) \text{ GeV} . \tag{2}$$

The total uncertainty is dominated by the statistical term. The systematic uncertainty is divided into different terms where the dominant one is related to the electron/muon energy/momentum scales and resolutions (denoted as “scale”). Other systematic sources have only a very minor effect on the mass measurement. The results of the Higgs boson mass measurements performed by the individual experiments as well as the combined values are shown in figure 2.

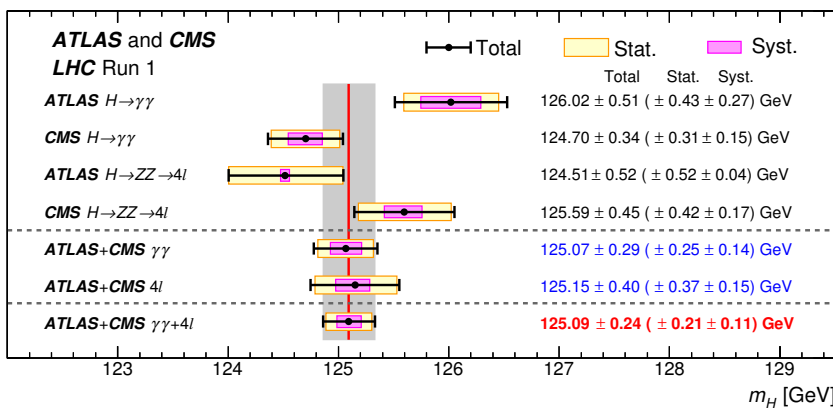


Fig. 2. Higgs boson mass measurements using the ATLAS and CMS detectors. Taken from Ref. [8].

Compatibility tests have been performed to check the consistency between measurements in different decay channels and between the two experiments. The four measurements (two different decay channels in two experiments) have shown an agreement within 2σ . The combined measurement of the Higgs boson mass improves the results of the individual experiments and leads to currently highest precision.

4. Higgs couplings and signal strength

Results of the combined ATLAS and CMS measurement of the Higgs boson production and decay rates using Run 1 data [12] are presented in this section. The production modes, which have been studied, are gluon fusion (ggF), vector boson fusion (VBF), and associated production with vector bosons (VH) and with a top–anti-top pair (ttH). The decays involving

a coupling to bosons ($H \rightarrow ZZ \rightarrow 4\ell$, $H \rightarrow WW \rightarrow \ell\nu\ell\nu$, $H \rightarrow \gamma\gamma$) and to fermions ($H \rightarrow \tau\tau$, $H \rightarrow \mu\mu$, $H \rightarrow bb$) have been considered. The Higgs boson mass has been fixed to $m_H = 125.09$ GeV.

4.1. Measurements of the signal strengths

The signal strength parameter for the given production and decay mode ($i \rightarrow H \rightarrow f$) is defined as

$$\mu_i^f = \mu_i \times \mu^f = \frac{\sigma_i}{(\sigma_i)_{\text{SM}}} \times \frac{\text{BR}^f}{(\text{BR}^f)_{\text{SM}}}, \quad (3)$$

where σ_i and BR^f are the respective measured production cross section for $i \rightarrow H$ and branching ratio for $H \rightarrow f$. The subscript ‘‘SM’’ refers to their respective Standard Model predictions, $\mu_i^f = 1$ by definition in the SM.

The simplest assumption is to restrict the signal strength parameters μ_i and μ^f to the same value for all production processes and decay modes. In this case, a global signal strength parameter has been extracted from data with the best fit value of $\mu = 1.09_{-0.10}^{+0.11}$. The largest uncertainties come from the statistical term and the theoretical uncertainty on the gluon fusion cross section. The measured signal strength is consistent with the SM expectation within 1σ .

The strict assumption of the global signal strength is very model-dependent. This assumption has been relaxed separately for the production cross sections and the decay branching ratios to allow tests in a less model-dependent way. First, the Higgs boson branching ratios are fixed to the SM values ($\mu^f = 1$) and the five production modes have been treated with independent signal strengths as shown in figure 3 (a). Next, the production cross sections are assumed to be the SM one, while the decay signal strengths have been fitted, see figure 3 (b). The unitarity ($\Sigma \text{BR}^f = 1$) is ensured by the fact that the total width is included in the couplings parametrisation.

The observed significances of the VBF production process and of the $H \rightarrow \tau\tau$ decay has been measured to be at the level above 5σ . The measured significance of the VH production process has been above 3σ in the combination. The largest difference with respect to the SM expectations has been found for the ttH production where the combined significance is 4.4σ and only 2.2σ is expected.

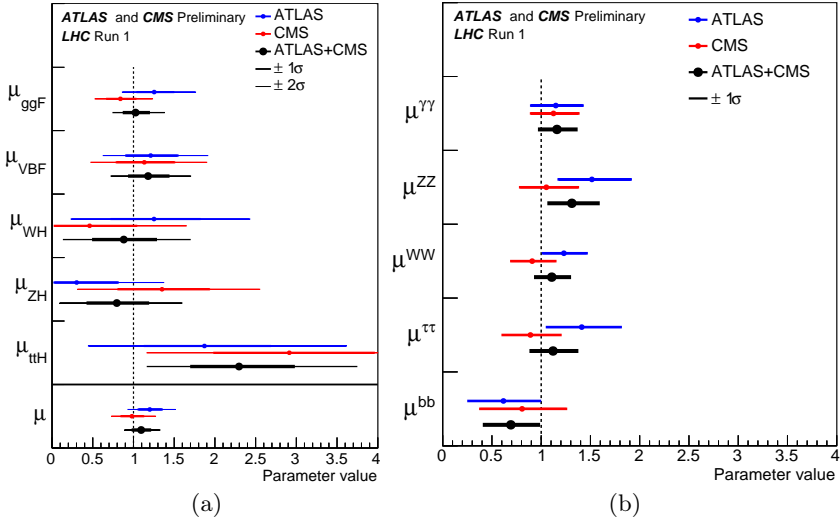


Fig. 3. Best-fit results for the production (a) and decay (b) signal strength parameters. Taken from Ref. [12].

4.2. Constraints on the Higgs boson couplings

An example of an analysis of a more generic model based on the coupling modifiers is discussed here. The coupling modifiers are used to interpret the LHC data using specific modifications of the Higgs boson couplings related to new physics beyond the SM. The measured signal yield can be parametrised as

$$\sigma_i \times \text{BR}^f = \frac{\sigma_i(\vec{\kappa}) \Gamma^f(\vec{\kappa})}{\Gamma_H}, \tag{4}$$

where Γ_H denotes the total width of the Higgs boson and Γ^f the partial width of the Higgs boson decay to the final state f . The symbol $\vec{\kappa}$ stands for a set of coupling modifiers which are used to parametrise potential deviations from the SM predictions. The modifiers $\vec{\kappa}$ are defined for a given production process or decay mode denoted j as follows

$$\kappa_j^2 = \sigma_j / \sigma_j^{\text{SM}}, \quad \text{resp.} \quad \kappa_j^2 = \Gamma^j / \Gamma_{\text{SM}}^j. \tag{5}$$

By definition, all κ_j values are positive and equal to unity in the SM. The SM cross section and branching ratios are taken to the best knowledge in the higher-order QCD and EW corrections.

The rates of the Higgs boson production in the various decay channels are inversely proportional to the Higgs boson width, which is sensitive to invisible or undetected Higgs boson decays predicted by many beyond Standard Model theories (BSM). The assumptions on the Higgs boson width are necessary. Two scenarios are discussed in this section. In the first one, the Higgs boson is not allowed to have any BSM decay ($\text{BR}_{\text{BSM}} = 0$). In the second one, the BR_{BSM} parameter is left free, but it assumes that $\kappa_W \leq 1$ and $\kappa_Z \leq 1$. The BSM physics might occur in the loops of the $gg \rightarrow H$ production and in the $H \rightarrow \gamma\gamma$ decay. These processes are particularly sensitive to loop contributions from new heavy particles. These can be probed by using the effective coupling modifiers. The parameters of interest are seven independent coupling modifiers (one for each SM particle involved in the production processes and decay channels studied) plus BR_{BSM} in the case of the second fit. The results of the fits are shown in Table I for both scenarios.

TABLE I

Coupling modifiers for two scenarios allowing BSM contribution. Taken from Ref. [12].

Parameter	ATLAS+CMS Measured	ATLAS+CMS Expected uncertainty	ATLAS Measured	CMS Measured
Parameterisation assuming $\text{BR}_{\text{BSM}} = 0$				
κ_Z	$1.03^{+0.11}_{-0.11}$	$+0.10$ -0.11	$1.00^{+0.14}_{-0.14}$	$1.07^{+0.17}_{-0.18}$
κ_W	$0.91^{+0.10}_{-0.10}$	$+0.10$ -0.11	$0.92^{+0.13}_{-0.13}$	$0.90^{+0.15}_{-0.15}$
κ_t	$1.43^{+0.23}_{-0.22}$	$+0.26$ -0.32	$1.31^{+0.30}_{-0.32}$	$1.56^{+0.34}_{-0.32}$
κ_τ	$0.88^{+0.13}_{-0.12}$	$+0.16$ -0.15	$0.97^{+0.19}_{-0.17}$	$0.82^{+0.19}_{-0.17}$
κ_b	$0.60^{+0.18}_{-0.18}$	$+0.25$ -0.24	$0.61^{+0.26}_{-0.26}$	$0.61^{+0.27}_{-0.26}$
κ_g	$0.81^{+0.11}_{-0.10}$	$+0.17$ -0.14	$0.94^{+0.18}_{-0.15}$	$0.70^{+0.15}_{-0.13}$
κ_γ	$0.92^{+0.11}_{-0.10}$	$+0.12$ -0.12	$0.88^{+0.15}_{-0.14}$	$0.96^{+0.17}_{-0.15}$
Parameterisation assuming $\kappa_V \leq 1$				
κ_Z	$1.00_{-0.08}$	-0.11	$1.00_{-0.14}$	$1.00_{-0.12}$
κ_W	$0.90^{+0.09}_{-0.09}$	-0.11	$0.92^{+0.08}_{-0.13}$	$0.86^{+0.14}_{-0.13}$
κ_t	$1.42^{+0.23}_{-0.22}$	$+0.27$ -0.32	$1.31^{+0.34}_{-0.32}$	$1.53^{+0.35}_{-0.31}$
κ_τ	$0.87^{+0.12}_{-0.11}$	$+0.14$ -0.15	$0.97^{+0.21}_{-0.17}$	$0.80^{+0.18}_{-0.16}$
κ_b	$0.57^{+0.16}_{-0.16}$	$+0.19$ -0.23	$0.61^{+0.24}_{-0.26}$	$0.55^{+0.24}_{-0.23}$
κ_g	$0.81^{+0.13}_{-0.10}$	$+0.17$ -0.14	$0.94^{+0.23}_{-0.15}$	$0.70^{+0.16}_{-0.13}$
κ_γ	$0.90^{+0.10}_{-0.09}$	$+0.10$ -0.12	$0.88^{+0.15}_{-0.14}$	$0.93^{+0.15}_{-0.13}$
BR_{BSM}	$0.00^{+0.16}$	$+0.18$	$0.00^{+0.26}$	$0.00^{+0.23}$

No deviations from the SM predictions have been observed for all parametrisations considered.

5. Higgs spin and CP

The study of the spin and parity of the Higgs boson has been performed in ATLAS [13] and CMS [14] collaborations. In the following, the details of the CMS measurements are given.

The spin and parity measurements have been performed in $H \rightarrow ZZ \rightarrow 4\ell$, $H \rightarrow \gamma\gamma$ and $H \rightarrow WW \rightarrow \ell\nu\ell\nu$ decay modes using LHC data from Run 1. In the case of the resonance with a non-zero spin, its polarisation depends on the production mechanism. Consequently, a non-trivial correlation of the kinematic distributions of production and the decay would be observed for a resonance with non-zero spin. In contrast, there is no such direct correlation due to polarisation for a spin-zero resonance. Moreover, the kinematics of the leptons in the $VV \rightarrow 4\ell$ or $VV \rightarrow \ell\nu\ell\nu$ (V denotes either Z or W) decay is affected by the initial polarisation of the resonance and the tensor structure of the HVV interactions.

The full kinematic information is available for the $H \rightarrow ZZ \rightarrow 4\ell$ decay. The kinematics is commonly described by five angles (figure 4) and three invariant masses (masses of the two dilepton pairs and of the four-lepton system). The kinematic variables are measured with small experimental uncertainties in this channel. In the case of the $H \rightarrow WW \rightarrow \ell\nu\ell\nu$ decay, a part of the kinematic information is lost due to the two neutrinos. However, the V - A nature of the $W \rightarrow \ell\nu$ coupling leads to more pronounced kinematic effects.

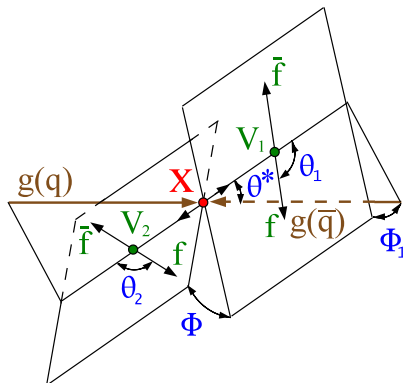


Fig. 4. Illustration of the angles used in the spin-parity analysis of the Higgs boson decay to two vector bosons. The two production angles θ^* and ϕ_1 are shown in the X rest frame (X stands either for a Higgs boson or an exotic particle). The three decay angles θ_1 , θ_2 and ϕ are defined in the V rest frames. Taken from Ref. [14].

The spin-parity analysis of the $H \rightarrow \gamma\gamma$ decay has been studied in the context of the exotic spin-two hypothesis tested with respect to the SM hypothesis. However, only one angle θ^* out of the five shown in figure 4 has been used in this case. Its distribution is isotropic in the boson frame for any spin-zero model and, therefore, such models cannot be distinguished.

The parametrisation of the multidimensional distribution as a function of the parameters of interest would be required in the analysis of a large number of observables (eight in the case of the $H \rightarrow ZZ \rightarrow 4\ell$ channel). This is rather difficult due to strong correlations between the observables. An alternative method, based on a matrix element likelihood approach, is used in order to reduce the number of observables. This retains full information for the measurements of interest. In this approach, the kinematic information is stored in a discriminant which is designed for the separation of the background, the alternative signal components and interference between those components. This approach has been used in the $H \rightarrow ZZ \rightarrow 4\ell$ channel where different spin hypotheses are tested. A similar approach is also possible in the $H \rightarrow WW \rightarrow \ell\nu\ell\nu$, but the construction of the discriminants is more challenging because of the presence of unobserved neutrinos.

Using the above approaches, a wide range of spin-two models has been excluded at a confidence level of 2.5σ or higher. Any mixed-parity spin-one state has been excluded in the ZZ and WW modes at a confidence level greater than 4σ . All observations are consistent with the expectations for the Standard Model Higgs boson with the quantum numbers $J^{PC} = 0^{++}$. Similar conclusions have been drawn by the ATLAS experiment, details of the analysis can be found in Ref. [13].

6. Cross-section measurements at $\sqrt{s} = 13$ TeV

The strategy of analysing first data at the centre-of-mass energy of 13 TeV differs between the ATLAS and CMS experiments. Whereas the CMS Collaboration plans to re-discover the Higgs boson at 13 TeV and leaves the crucial signal regions blinded until sufficient statistics is collected, the ATLAS experiment has measured the Higgs boson production cross sections in the discovery channels $H \rightarrow \gamma\gamma$ [16] and $H \rightarrow ZZ \rightarrow 4\ell$ [15]. The latter measurements are discussed in this section.

The total cross section σ_{tot} can be expressed as

$$\sigma_{\text{tot}} = \frac{N_{\text{S}}}{A C B L_{\text{int}}}, \quad (6)$$

where N_{S} is the number of observed signal events, L_{int} stands for the integrated luminosity, B is the branching ratio of the considered Higgs boson

decay, A is the kinematic and geometric acceptance in the fiducial region, and C is a detector correction factor which accounts for trigger, reconstruction and identification efficiencies and reconstruction resolution.

The signal yield in the $H \rightarrow \gamma\gamma$ channel is estimated from the fit of the signal and background model. The signal model is described by the sum of a Crystal Ball and a Gaussian function. The steeply falling background contribution is fitted by an analytical function based on the templates built from the fast simulation samples. The distributions of the diphoton invariant mass from these templates are fitted in the same range as the data with a signal plus a background model. Since no signal is present in those background-only samples, the resulting number of signal events from fits is taken as an estimate of the bias in a particular background model under test. Only models with a reasonably small bias are taken into account. The exponential of a second order polynomial fulfils the required conditions on the background model. The extracted (expected) signal yields are $N_S = 113 \pm 74(\text{stat.})_{-25}^{+43}(\text{syst.})$ ($N_{\text{exp}} = 143 \pm 71(\text{stat.})_{-6}^{+39}(\text{syst.})$).

The main background in the $H \rightarrow ZZ \rightarrow 4\ell$ channel is the non-resonant ZZ^* diboson production. Monte Carlo simulations are used for the prediction of this background. The normalisation is checked in the phase space outside the signal region defined by $m_{4\ell} < 110$ GeV and $m_{4\ell} > 140$ GeV. Smaller but non-negligible background contributions come from the Z +jets and $t\bar{t}$ processes. Their normalisation is extracted by data-driven methods in the full mass region. Four events are observed in the narrow mass window of $118 < m_{4\ell} < 129$ GeV, while 4.57 ± 0.54 signal and 2.08 ± 0.20 background events are expected. The invariant mass spectrum is shown in figure 5.

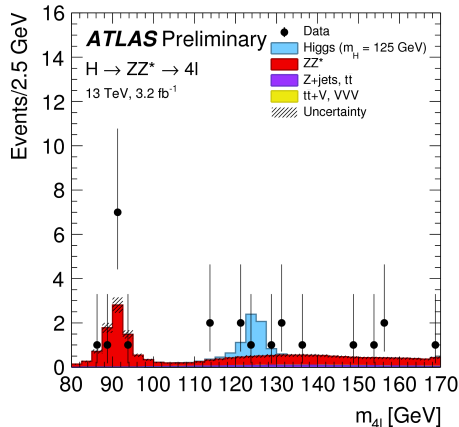


Fig. 5. Invariant mass spectrum measurement of the four lepton system in the $H \rightarrow ZZ \rightarrow 4\ell$ channel using the ATLAS detector. Taken from Ref. [15].

The results of the two cross-section measurements and their combination together with results from Run 1 are shown in Table II. The compatibility of the combined measurement at 13 TeV and the SM prediction [18] has been found to be 1.3σ .

TABLE II

ATLAS measurements of the total $pp \rightarrow H$ cross sections at different centre-of-mass energies together with the theoretical prediction. Taken from Ref. [17].

Total cross section [pb]	7 TeV	8 TeV	13 TeV
$H \rightarrow \gamma\gamma$	35_{-12}^{+13}	$30.5_{-7.4}^{+7.5}$	40_{-28}^{+31}
$H \rightarrow ZZ \rightarrow 4\ell$	33_{-16}^{+21}	37_{-8}^{+9}	12_{-16}^{+25}
Combination	$34 \pm 10(\text{stat.})_{-2}^{+4}(\text{syst.})$	$33.3_{-5.3}^{+5.5}(\text{stat.})_{-1.3}^{+1.7}(\text{syst.})$	$24_{-17}^{+20}(\text{stat.})_{-3}^{+7}(\text{syst.})$
Theoretical expectation	17.5 ± 1.6	22.3 ± 2.0	$50.9_{-4.4}^{+4.5}$

7. Conclusions

Several measurements of the Higgs boson properties using proton–proton data from Run 1 are discussed in this paper. The combined measurement of the Higgs boson mass using the ATLAS and CMS detectors provides the currently most precise value of $m_H = 125.09 \pm 0.24$ GeV. A combined ATLAS and CMS result is available also for the Higgs boson couplings and signal strength measurements. The global signal strength has been found to be $\mu = 1.09_{-0.10}^{+0.11}$ which is in a good agreement with the SM expectations. Several parametrisations allowing contributions from particles beyond SM have been tested, but no evidence of any deviation from the SM has been found. The measurement of the spin and parity of the Higgs boson performed by both ATLAS and CMS experiments have each shown a good agreement with a SM-like Higgs boson with $J^{PC} = 0^{++}$.

The preliminary cross section of the Higgs boson production at the centre-of-mass energy of 13 TeV has been measured in ATLAS. The measured cross sections again show agreement with the SM predictions within the uncertainties. More collisions data are expected to be delivered in Run 2 during next years and these will provide yet more precise measurements.

I thank CERN for the very successful operation of the LHC, as well as the support staff from our institutions without whom ATLAS and CMS could not be operated efficiently. I would like to thank all my colleagues from ATLAS and CMS experiments who were involved in the presented analyses. I would like to acknowledge the support of MSMT CR, Czech Republic.

REFERENCES

- [1] Atlas Collaboration, *JINST* **3**, S08003 (2008).
- [2] CMS Collaboration, *JINST* **3**, S08004 (2008).
- [3] F. Englert, R. Brout, *Phys. Rev. Lett.* **13**, 321 (1964).
- [4] P.W. Higgs, *Phys. Lett.* **12**, 132 (1964).
- [5] P.W. Higgs, *Phys. Rev. Lett.* **13**, 508 (1964).
- [6] ATLAS Collaboration, *Phys. Lett. B* **716**, 1 (2012).
- [7] CMS Collaboration, *Phys. Lett. B* **716**, 30 (2012).
- [8] ATLAS and CMS collaborations, *Phys. Rev. Lett.* **114**, 191803 (2015).
- [9] ATLAS and CMS collaborations, ATL-PHYS-PUB 2011-11.
- [10] G. Cowan, K. Cranmer, E. Gross, O. Vitells, *Eur. Phys. J. C* **71**, 1554 (2011).
- [11] CMS Collaboration, *Eur. Phys. J. C* **74**, 3076 (2014).
- [12] ATLAS and CMS collaborations, ATLAS-CONF-2015-044, CMS-PAS-HIG-15-022.
- [13] ATLAS Collaboration, *Eur. Phys. J. C* **75**, 476 (2015).
- [14] CMS Collaboration, *Phys. Rev. D* **92**, 012004 (2015).
- [15] ATLAS Collaboration, ATLAS-CONF-2015-059.
- [16] ATLAS Collaboration, ATLAS-CONF-2015-060.
- [17] ATLAS Collaboration, ATLAS-CONF-2015-069.
- [18] R. Andersen *et al.*, *Handbook of LHC Higgs Cross Sections: 3. Higgs Properties*, 2013.